INTERNATIONAL INSTITUTE OF EDUCATIONAL RESEARCH & DEVELOPMENT

International Conference on Researches in Science and Technology

(ICRST-20)

Accra, Ghana

09th-10th July, 2020

International Institute of Education, Research and Development

www.iierd.org

Determination of Rainfall Attenuation at Millimeter Wave Band for the Design of 5G and Higher Bandwidth Radio Equipment for Terrestrial Paths in The Tropical Region

[1] Ibe Osita, [2] E. F. Nymphas

[1][2] Department of Physics, University of Ibadan

Abstract— **Millimeter Wave (mmW) radio systems operating at 30 to 300GHz band provides higher bandwidth, frequency reuse and communications security. With the available wide bandwidth, millimeter wave equipment is capable of achieving 10 Gbps full duplex capacities. The mean annual 1-minute RR (mm/hr) ranged from 87.25 in the coastal region to 51.0mm/hr in semi-arid region. The ITU-R predicted RR ranged from 109.10mm/hr in the coast to 91.90mm/hr in the semi-arid region. The ITU-R over-estimated the rain rate by 23.83% in the semi-arid region while at the coastal region, it was over-estimated by 12.47%. The highest value of specific attenuation (γ_R) at horizontal polarization (H_p) and vertical polarization (V_p) for the two regions occurred at 120 and 150GHz MWFs and $\gamma_R H_P > \gamma_R V_P$. The clear signal band at 20km Path length were estimated to be 40 and 45GHz across the regions, while the predicted value by ITU-R is also 40GHz. However, the ITU-R over predicted the value of attenuation at this frequency band by 13.16% and 35.29% at the coastal and semi-arid locations respectively. included 150GHz which overlaps with 45GHz band. The path attenuation across the regions at 40GHZ ranged from 112.58dB to 164.14dB while at 45GHZ, it ranged from 122.02dB to 175.57.45dB. The range of the ITU predicted value of path attenuation at 40GHz and 45GHz were 170.20dB to 192.18dB and 181.83 dB to 204.43dB respectively.**

Index Terms— **Rain rates, Rain attenuation, Path attenuation, Propagation frequency, ITU-R**

I. INTRODUCTION

The pressing need for developing diversities of and fast communication systems in-order to satisfy the yearnings of telecommunication companies and the general public has pushed scientists and Engineers to explore for the potential use of higher bands (microwave and millimeter wave) of the electromagnetic spectrum (Karmakar, 2010; Sakir, 2014; Ghiani et al., 2017). The preference for these bands is premised on the availability of large bandwidth, higher channel capacities, high speed data transmission, miniaturized device size (antenna with other equipment) and expanse in the availability of spectrum (Owolawi*et al.,* 2009, 2012, Ramakrishna *et al.,* 2014). Millimeter wave also called "mmWave" or Extremely High Frequency (EHF) is the highest radio frequency band in practical use. It is the next band above microwave or Super High Frequency (SHF) and lies between 30-300GHz of the electromagnetic spectrum. It corresponds to wavelengths of between 1 to 10 millimeter (Skolnik, 1970, Bhartia*et al.,* 1984) and is characterized by narrow beam width, wide bandwidth spectrum and high frequency re-use potential (Owolawi*et al.,* 2009). When compared to microwaves (cm), mmWaves have considerably broader bandwidths, small component/subsystem sizes, light weight, reduced multipath effects, reduced vulnerability to jamming, better sea clutter operability and selective atmospheric attenuation (Rao, 2010).

Millimeter wave is an ideal candidate for certain applications such as provision of higher data rates in supporting applications such as Voice-Over-IP, local network remote access, inter- active audio-visual conferencing, wireless internet access of high speed, multimedia information broadcasting and file transfer (Marcus et al., 2005; Owolawi, 2006; Owolawi*et al.,* 2012). The mm wave affords communication links that are densely packed, hence provides communication transmissions increased security and efficiency in spectrum utilization (FCC, 1997; Godara*et al.,* 2013). The utilization of millimeter wave frequency bands can permit telecommunication operators to increase traffic and ultimately reduce telecommunication costs.

With the available wide bandwidth, millimeter wave equipment is capable of achieving 10 Gbps full duplex capacities. This bandwidth is far beyond the capability of lower radio frequencies wireless technologies. The availability of this extraordinary amount of bandwidth enables radio propagation engineers to scale millimeter

wave wireless links up to 10 Gbps as demanded by market needs. As the demand for higher capacity links increases, millimeter wave technology is designed to meet the increasing demand for higher capacity links by using more efficient modulation schemes (Prasanna, 2008).Considering the increase in spectrum occupancy and higher bandwidth demand to accommodate complex radio access network evolution, the need to explore the merits of millimetric wave band has become imperative.

So far the design of radio communication equipment has been based on predicted rain rate and rain attenuation from the International Telecommunication Union-Radio (ITU-R) model. However, such equipment does not perform optimally in the tropics because rainfall in this region is more intense with larger drop sizes than those in the temperate regions on which the ITU-R model was based. The severity of rainfall impairments is more predominant in the equatorial and tropical climates which are characterized by rainfall events that are intense with larger raindrop sizes (Nandi et al., 2019; ITU-R, 2003; Ajayi*et al.,* 1996). The percentage availability of mm wave link in a given location is determined by the characteristics of rainfall at the location of interest (Prasanna, 2008). The lack of appropriate rainfall data (1-min) in the tropics for incorporation into and possible modification of the ITU-R model has led to the failure of radio link equipment designed based on the ITU-R model in the region due to the differences in the rainfall structure (Bryant, 1998, Ajayi*et al.,* 1996; Ibe and Nymphas, 2020). The study of rain attenuation phenomenon in the tropics is therefore imperative for efficient planning of millimetre wave terrestrial wireless communication systems and utilization (Vaclav *et al*. 2010). This study therefore aims at investigating rain attenuation at coastal and semi-arid climates in Nigeria. The performance of the ITU-R model in estimating path attenuation was compared with the Crane (1996) and Moupfouma (1984) models. The adequacy of the ITU-R model in estimating specific attenuation was also assessed.

II. METHODOLOGY

2.1 Data Source

The four years 5-min rainfall data was collected from Tropospheric Data Acquisition Network (TRODAN) setup, a project put forward by the Nigerian Centre for Atmospheric Research (CAR). Real-time meteorological data was collected from different locations across Nigeria. TRODAN serves as a tool for reliable terrestrial and satellite communication networks planning, weather prediction, agricultural usage and hydrological purposes. The detailed description of the equipment used at each TRODAN station and their characteristics is given in Ibe and Nymphas (2017). Brief characteristics of the two stations selected for this study is given in Table 1.

Table 1: The climatological characteristics of the stations used for this study

Sites	Coordinates	Altitude (m)	Average annual rainfall (mm/yr)	Climatic Region
Port Harcourt	4.75°N 7.00°E	468	1684.13	Coastal
Makurdi	7.73°N 8.54°E	140	734.38	Semi-arid

2.2 Data Analysis

2.2.0 Conversion of 5-min rainfall rate to 1-minute integration time

Rainfall attenuation is comparable to rainfall rate in millimeter per hour (mm/hr) rather than rainfall in millimeter (mm), hence it is necessary to first convert the available rainfall data into rainfall rate. The expression required for the conversion is as follows:

$$R_D = L^* \frac{60}{T} \text{ (mm/hr)} \quad (1)$$

Where L is the maximum rainfall (mm) and $R_D$applies to the rainfall rate (mm/hr) and for time interval T (min) (Kestwal et al., 2014; Ali et al., 1986). Rainfall rate that exceeds the integration time of 1-minute under-estimates measured rain rate (Chun, 2013). The fluctuation caused by rain gauge measurement process is resolved by 1-minute accumulation. Several models have been proposed for the conversion of rain rate from higher integration time to 1-minute integration time. Among these models are Flavin (1981), Chebil and Rahman (1999), Joo et al., (2002), Moupfouma and Martins (1995), Ojo et al., (2016), Ajayi et al., (1996) and Semire et al.,(2012). However, most of these models are either restricted to a fixed integration time or are characterised by location dependent regression coefficients, hence the need for a model that is suited for arbitrary integration times and independent of location. The Lavergnat and Gole (LG) (1998) model which is a semi-empirical physical stochastic model performs best overall integration time and climatic regions (Ojo et al., 2016). The model was developed through the application of stochastic process for time interval between rain drops. The advantage of the method is that it allows a conversion between any integration times. The conversion of rain rate of higher integration time to 1-minute integration time as recommended by ITU-R was achieved using the LG model which was found suitable for this region among other models and is given as

$$Q_c(r,t) = K^{\xi-1} Q_c\left(rk^{\xi-1}, kt\right) \quad (2)$$

where $Q_c(r,t)$ implies the function of rain rate (r) cumulative probability that would be captured with a rain measuring gauge of integration time t. Equation (2) thus allows a rain rate distribution observed in all the locations of the study area using an integration time kt, to be changed into one that would have prevailed for an integration time t. Equation (2) was used to convert the TRODAN data of 5-min into 1-min integration after which further analysis were carried out (Ibe and Nymphas (2020).

2.2.1: Determination of rain attenuation statistics

Rain induced attenuation can be predicted using rainfall Cumulative Distribution (CD) measured at a point (Moupfouma,1984). It can also be predicted by using the concept of mean rain rate over the propagation paths and the length of the effective path coverage of the radio signal. Furthermore, some authors use the reduction factor concept of a time percentage to multiply the point rainfall rate and then use the reduction coefficient to multiply the actual length (Moupfouma, 1984). However, rain rate is not constant along link path and over the year. As a result, CD of rainfall across the year has been preferred for Predicting rain attenuation (Sakir, 2014). Several models for predicting rain attenuation due to rain on earth-space path exist in literature. They are generally used for estimating rain attenuation where adequate data is not available. To get the CD from the annual rainfall amount, there are a number of rain rate prediction models which include the Moupfouma (1984) model, Crane Global model (1996) and ITU-R (2015). These models require rain rate ($R_{0.01}$) at the 0.01% exceedance at 1-minute integration time. These models are briefly discussed below.

2.2.2 ITU-R p. 530-17 (2017) Model

The ITU-R model has been widely accepted by the international propagation community for estimating long term statistics of rain attenuation at high frequencies in most regions of the world. The ITU - R P.530-**17** (**2017**) recommendation has given some techniques for extended period of rain induced attenuation estimation. The specific attenuation, Y_R (dB/km), is given by the power law

$$\gamma_R = kR^{\alpha} \quad (3)$$

where k and α are functions of frequency (GHz) ranging from 1GHz to 1000GHz and are expressed as

$$k = \frac{\left[k_H + k_v + (k_H - k_v)\cos^2\theta\cos 2\tau\right]}{2} \quad (4)$$

and

$$\alpha = \frac{\left[k_H\alpha_H + k_v\alpha_v + (k_H\alpha_v - k_H\alpha_v)\cos^2\theta\cos 2\tau\right]}{2k} \quad (5)$$

where θ is the elevation angle and τ is the polarization tilt angle measured relative to the horizontal plane. The subscripts H and v stands for horizontal and vertical polarization respectively.

The effective path length (d_{eff}) is computed by multiplying the actual path length d by a distance factor r given as

$$r = \frac{1}{0.477 d^{0.633} R_{0.01}^{0.073\alpha} f^{0.123} - 10.579(1-\exp(-0.024d))} \quad (6)$$

where f(GHz) is the frequency and α is as given by Eqn.(5). The path length $(A_{0.01})$ exceeded at 0.01% of time is expressed as

$$A_{0.01} = \gamma_R d_{eff} = \gamma R dr(dB) \quad (7)$$

When the attenuation at other percentages of time p if desired, say in the range 0.001% to 1%, the power law given by Eqn.(8) is used.

$$\frac{A_p}{A_{0.01}} = C_1 p^{-(C_2 + C_3 \log_{10} p)} \quad (8)$$

where

$$C_1 = \left(0.07^{C_0}\right)\left[0.12^{(1-C_0)}\right] \quad (9)$$

$$C_2 = 0.855C_0 + 0.546(1-C_0) \quad (10)$$

$$C_3 = 0.139C_0 + 0.043(1-C_0) \quad (11)$$

The value of C_o in Eqs.(9-11) take diffèrent values depending on the frequency. It takes the value in Eqn.(12) for the frequencies specified.

$$C_0 = \begin{cases} 0.12 + 0.4\left[\log_{10}(f/10)^{0.8}\right] & f \geq 10\ GHz \\ 0.12 & f < 10\ GHz \end{cases} \quad (12)$$

The prediction procedure outlined above is considered to be valid in all parts of the world at least for frequencies up to 100 GHz and path lengths up to 60 km (ITU - R P.530-**17**, **2017**)

2.2.3: Moupfouma (1984) Model

Moupfouma (1984) propose an empirical model for predicting line-of-sight terrestrial radio links attenuation by rain given as

$$A\ (dB) = kR^{\alpha}L_{eff} \quad (13)$$

The parameters k and □are the regression reduction coefficients which depend on the frequency and polarization. The effective path length L_{eff} is expressed as

$L_{eff} = rl$ (14)

where l is the actual path length (km). The coefficient, r, is given as

$$r = \frac{1}{1+cl^{m}} \quad (15)$$

From Equation (15), the parameters C and m depends on the probability level p (in percentage), the frequency of the radio link and the length of its path respectively. The attenuation induced by rain A (dB) at rainfall rate R was calculated at the same time percentage. This model uses well known fitting procedures from experiments with radio links at 1.3km to 58km path length and frequency range of 7GHz-38GHz at tropical/subtropical and temperate locations.

2.2.4: Crane Global Model

This model was developed for use on terrestrial paths. The model was based on the variation of atmospheric temperature, geophysical observations, rain structure and rain rate (Crane, 1996). Crane (1996) assumed that for point rain rates in excess of 25mm/hr, the probability of their occurrence were independent of path length over distances greater than 10km. This enhances a sufficient sample size at a path length of 22.5km. According to Shebami (2017), this assumption was based upon experience with weather radar data and it was in agreement with observations at path lengths of 10, 15, 20 and 22.5km and with power law approximations. This model was implemented by Crane using a piecewise representation of the path profile by exponential functions. The resulting attenuation model for a given rain rate is given by Crane (1996) as

$$A_T(R,D) = \gamma(R)\left(\frac{e^{y\delta(R)}-1}{y} + \frac{e^{ZD}-e^{Z\delta(R)}}{z}e^{\alpha\beta}\right)$$

$$\delta(R) < D < 22.5 \quad (16)$$

$$A_T(R,D) = \gamma(R)\left(\frac{e^{y\delta(R)}-1}{y}\right),$$

$$0 < D < \delta(R) \quad (17)$$

where γ(R) is as given by Eqn.(3)

III. RESULTS AND DISCUSSION

3.1 Accumulated Rainfall Distribution

Rainfall is one of the most discontinuous atmospheric phenomena with significant spatial and temporal variability (Sulochana et al., 2014) hence the need to obtain the cumulative distribution. The cumulative rainfall distribution (mm) was deduced from available rainfall data for the period of the study in the two locations under investigation on monthly and annual basis.

The annual and monthly accumulated rainfall distribution is presented in figures 1 and 2.

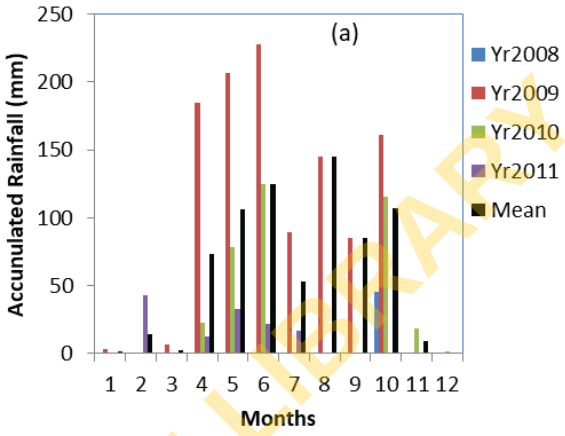

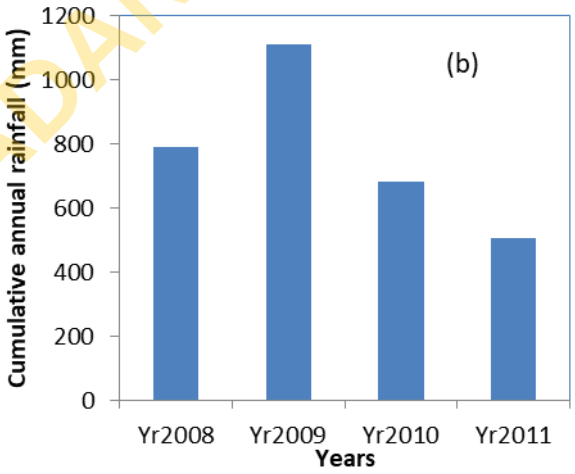

Figure1: Cumulative (a) monthly and (b) annual rainfall (mm) in semi-arid region

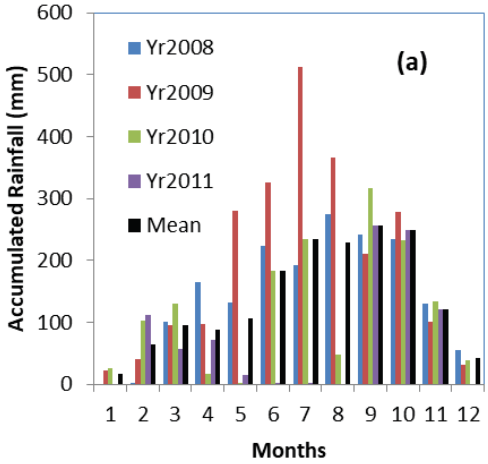

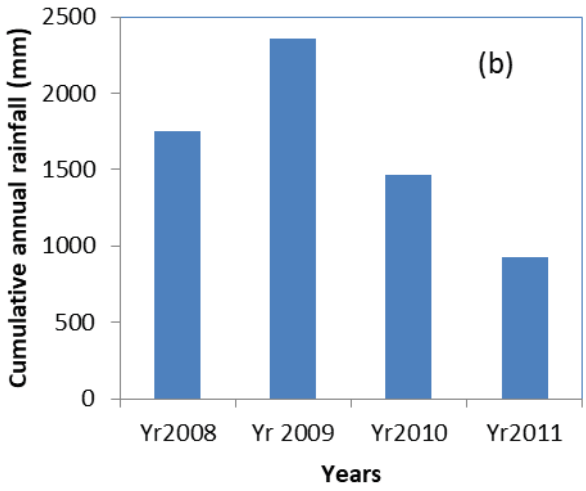

Figure 2: Cumulative (a) monthly and (b) annual rainfall (mm) in the coastal region

The situation at the semi-arid climatic region is shown in Figure 1. As can be seen in Figure 1a,the highest rainfall occurred in June 2009 with anaccumulated rainfall of 227.60mm.However, the month of August is characterized with the worst mean rainfall accumulation (145.30mm) for the period of study hence the worst month for radio wave propagation at the region. The year 2009 which recorded the highest rainfall accumulation of 1110.10mm is the worst year for radio link (Figure 1b). Figure 2 (a-b) presents the accumulated rainfall amount in the coastal climate. From Figure 2a, the month of July, 2009 recorded the highest monthly accumulated rainfall of 511.90 mm. The highest mean monthly accumulated rainfall amount (256.68 mm) was observed in September. Hence, the month of September was the worst calendar month for radio link at the region. Figure 2b is the annual accumulated rainfall for the study period. The year 2009 was observed as the worst year with a total rainfall accumulation of 2356.10 mm. Hence 2009 was the worst calendar year of a radio link at the coastal region.

3.2 Cumulative Distribution Function (CDF) of Rain Rates based on Different Integration times

Rainfall rate distribution is a function of sampling interval of rain gauge. Higher rain gauge sampling interval causes the under estimation of measured rain rate (Chun, 2013). One minute accumulation corrects the defects in rain measurements by gauges and presents values that are close to the ideal (Crane, 1996). Rainfall rates CDF gives an estimate of rainfall rates as a function of rain gauge sampling interval. The rain-gauge used for data collection at each location in the study area was configured to capture the rainfall data at 5 minutes integration time. The LG (1998) model was used to convert the 5 minutes rainfall data to 1-minuted which is the lowest compromise for attenuation determination (Fashuyi, 2006). The fact that rainfall measured at higher integration time underestimates rainfall rate is demonstrated in Fig. 3 which show the rainfall at 1- and 5-minutes integration time.

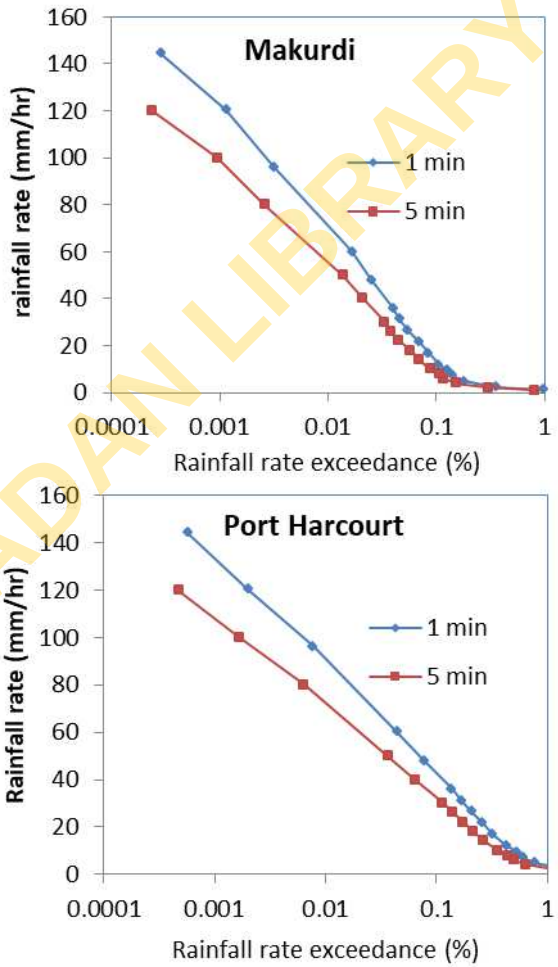

Figure 3: Rain rates distribution at 5-minutes and 1-minute integration time at Port Harcourt and Makurdi

The CDF of rainfall rate distribution at 1 and 5 minute integration time at the semi-arid and coastal region(Fig.3) shows that at 5 minutes integration time, rainfall rate at these regions were continually exceeded by 100mm/hr and 104.5mm/hr respectively at 0.001% while at 1- minute integration time, the exceedence was130mm/hr and 132mm/hr respectively. At 0.01% of exceedence at 5 minutes, the exceedance was59.5mm/hr and 71.0mm/hr respectively while at 1- minute integration time, the rainfall rate exceedence was 79.5mm/hrand 90.5mm/hrat the semi-arid and coastal areas respectively. At a higher percentage of exceedence (0.1%), rainfall rate of about 8mm/hr and 30mm/hr respectively was continually exceeded at 5-minutes integration time while at 1-minute,the exceedence

was about 15.5mm/hr and 45 mm/hrat the respective stations.

As can be observed from figure 3, rainfall rate is being under-estimated at integration time higher than 1- minute at all percentages of exceedance in all the climate regions. Considering the adverse effects of inaccurate rainfall rate prediction on system design, Olsen (1999) stressed the imperative for accurate propagation prediction as over-prediction can lead to costly system over-design whereas, the consequence of under-prediction can be unreliable system.

3.3: Annual Rainfall Rates Cumulative Distribution

The percentage of time of annual rain rate exceedance was used to obtain the rainfall rates cumulative distribution. As recommended by ITU-R P.837-7 (2017) on the precipitation characteristics suitable for modeling of signal propagation, consideration of the 0.01% rain rate exceedance which corresponds to 99.99 % radio signal availability and equivalent to about 53 minutes outage/year, 4.3minutes/month and 8.5 seconds/day is the recommended standard. The variation of the annual cumulative distribution of the averaged 1-minute integration time rainfall rate over the climatic regions are presented in Figure 4.

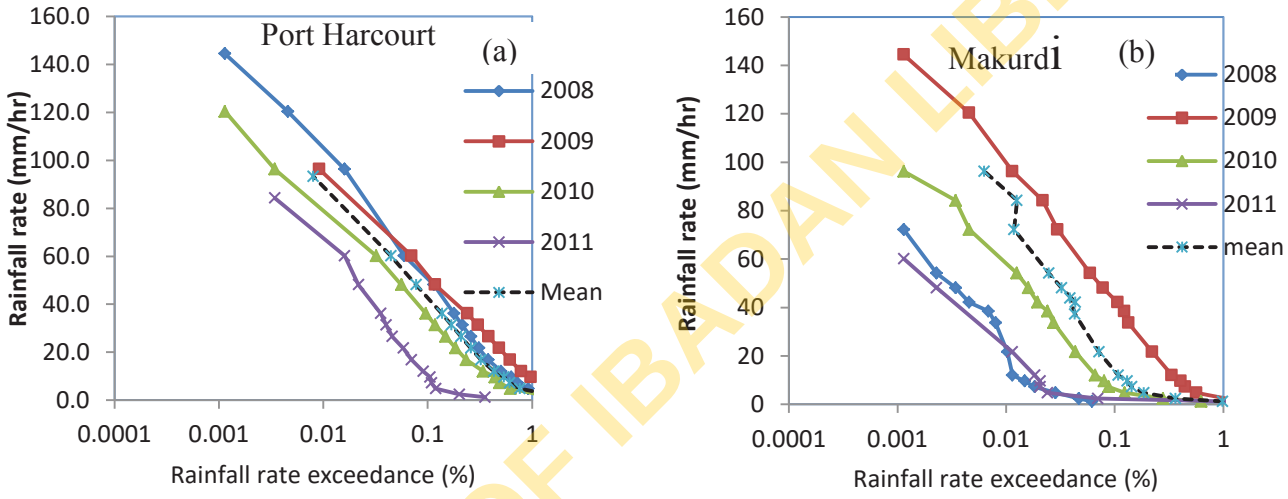

Figure 4: Annual Cumulative Distribution of Rainfall Rates over Port Harcourt and Makurdi

It can be observed from Figure 4, that as the percentage of time decreases, the rainfall rate increases and vice versa. At 0.01% of time, the year 2009 has the highest annual rainfall rate of 105.5mm/hrwhile the year 2008 has the least annual rainfall rate of 21.7mm/hr in Makurdi, the semi-arid region (Fig. 4b).At the coastal region, the year 2008 recorded the highest rainfall rate of about 110 mm/hr at the 0.01% of time while a minimum of rain rate of about 70 mm/hr was recorded in the year 2011.

3.4: Cumulative rainfall Rates and ITU-R Estimate

The International Telecommunication Union, Radio Sector (ITU-R) has provided a step by step approach for rain attenuation for terrestrial radio links. However, as averred by Abdulrahman et al. (2012) and Da SilvaMello et al., 2007, the ITU-R method does not perform well in tropical region, characterized by higher rainfall rates and greater radius of raindrops. The method is derived from data in temperate regions. For reliable prediction of rain attenuation at any location, the determination of the characteristics of rainfall of the study site is crucial (Owolawi et al., 2008). The comparison of ITU-R recommended rainfall rate at the locations considered is presented in the results below. As stated by Ojo *et al*., (2016), the LG (1998) model is the best over all other integration times and climate regions, hence the converted one minute integration time over all other locations are compared against the ITU-R recommendation. The ITU-R recommended percentage exceedences are: 1%,0.3%,0.1%,0.03%, 0.01%,0.003%, 0.001% and 0.0001%. Figure 5 and table 2 summarizes the situation at the regions.

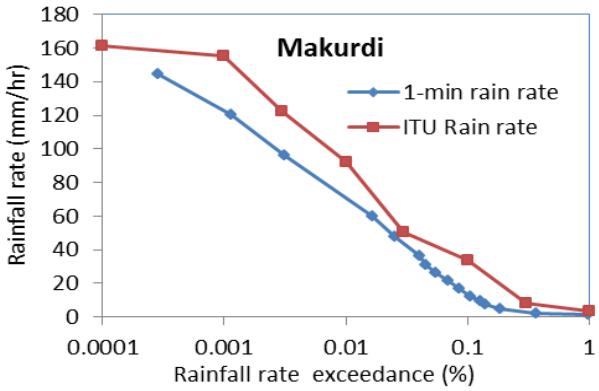

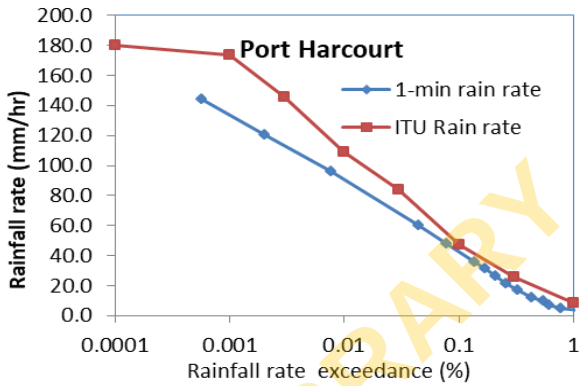

Figure 5: Cumulative Rain Rate Distribution over the semi-arid and coastal region

Table 2: ITU percentage of exceedance at different rainfall rates CD at the regions

ITU rain rate exceedance (%)	Makurdi			Port Harcourt		
	ITU-R	Observed	Diff. (%)	ITU-R	Observed	Diff (%)
1	3.23	3.20	0.93	8.15	-	-
0.3	8.04	8.00	0.50	25.57	16.85	34.10
0.1	33.70	9.60	71.51	47.50	45.00	5.26
0.03	50.23	50.50	0.53	83.95	66.00	21.38
0.01	91.90	70.00	23.83	109.10	95.50	12.47
0.003	122.61	88.00	28.23	145.54	118.00	18.92
0.001	155.40	121.50	21.81	173.40	135.00	22.15
0.0001	-	-	-	180.21	-	-

From Table 2 and Figure 5, it can be observed that in the semi-arid (Makurdi) and the coastal region (Port Harcourt), the rain rate is over-estimated by ITU-R in all the percentages of exceedance with the exception of 0.03% of time in the semi-arid region. At the 0.01% exceedance, ITU-R over-estimated the rain rate by 23.83% in the semi-arid region while at the coastal region, it was over-estimated by 12.47%.The implication of these result is that performance of communication equipment designed with ITU-R estimates, are bound to fall below expectation in the affected locations. The departure of ITU-R rain rate estimate from the observed values could lead to the design of systems that are unreliable in these tropical locations as corroborates by the findings of Olsen (1999).

3.5: Determination of Attenuation Characteristics

One of the major impediments facing the propagation of mm Waves in tropical regions is rain attenuation. When rain comes in contact with a radio link, it results in the absorption, scattering, and diffraction of radio waves which leads to increased transmission losses and a reduction in the received signal levels (Shayea et al., 2018). Rainfall is a natural occurrence and varies from time to time, year to year and location to location. Attenuation due to rainfall limits the performance of Line-Of-Sight (LOS) links above certain threshold frequency which can be as low as 7GHz in the tropics which are characterised by intense rainfall and larger raindrops (Moupfouma, 1984; Green, 2004).In the planning of LOS radio systems for terrestrial paths, accuracy is needed in the prediction of how rain would attenuate the signals(Segal, 1986). Three established models are utilized for the terrestrial paths rain attenuation prediction, these are: ITU-R, Crane Global and the Moupfouma methods (Fashuyi et al., 2007). The $R_{0.01}$ is defined as 0.01% rain rate exceedance in a location at 1-minute integration time. This percentage of rain rate exceedance was used for attenuation determination.

3.5.1 Specific Attenuation Computation

The specific attenuation γ, also referred to as attenuation per unit distance is essential for rain attenuation computation for terrestrial as well as earth-space paths(Olsen et al., 1978).The relationship between γ and rain rate (R) has been given as:

$$\gamma = kR^{\alpha} \tag{18}$$

where the parameters k and α are governed by the operating frequency. However, rainfall is not uniform all through the propagation path of the radio link as convective cells alternate with stratiform ones (Moupfoufam, 2009). The rain drops amount and size also vary spatially and

temporarily. This is why the equivalent propagation path length L_{eff} (eqn. 13) is often assumed to be uniform. Also, measuring these parameters in a part of the Earth is not sufficient for predicting attenuation for the whole path of radio link (Sakir, 2014). This calls for techniques that will cope with the temporal and spatial variation of rain characteristics. The Values of k and α were obtained for 30 to 300GHs frequency range. The specific attenuation, γ_R (dB/km) for the two eco-climatic zones used for the study were computed based on ITU-R P. 838-3 (2005) recommendation. Using the actual local rain data from these locations, the 0.01% (99.99%) rain rate exceedance ($R_{0.01}$) was determined for the period of study and the mean of the duration was obtained. Table 3 shows the statistics of rainfall rate cumulative distribution at 0.01%exceedance.

Table 3: Rain rate statistics at 0.01% exceedance

Locations	2008 (mm/hr)	2009 (mm/hr)	2010 (mm/ hr)	2011 (mm/hr)	Average (mm/hr)	ITUR (mm/hr)
Port Harcourt	106.00	98.00	77.50	67.50	87.25	109.10
Makurdi	22.00	100.00	58.00	24.00	51.00	91.90

The specific attenuation (γ_R) was calculated for both the horizontal and vertical polarization. The specific attenuation is known to increase with frequency up to around 100GHz and decreases at higher frequencies (Das and Maitra, 2010; Sakir, 2014). However, according to Diba (2017), specific attenuation can remain constant for frequency up to 150GHz and decreases afterwards. Figures 6 and 7 shows the plot of specific attenuation from the observed data and ITU-R predicted values for both horizontal and vertical polarization.

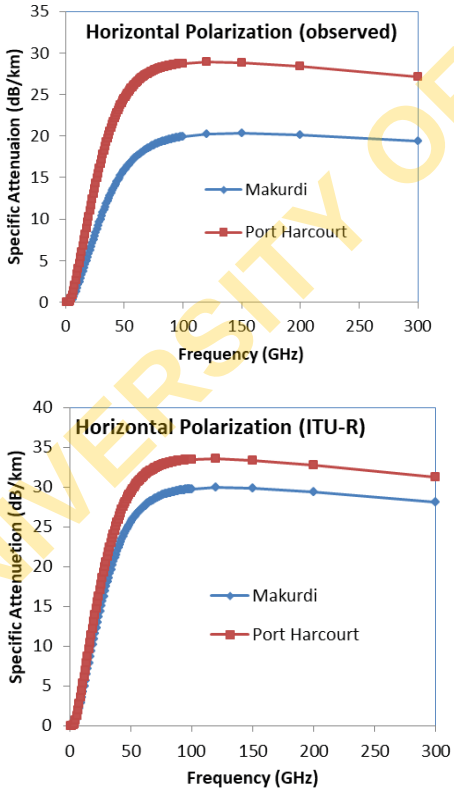

Figure 6: Specific rain attenuation versus frequency for horizontal polarization using observed and ITU-R rain rate data-

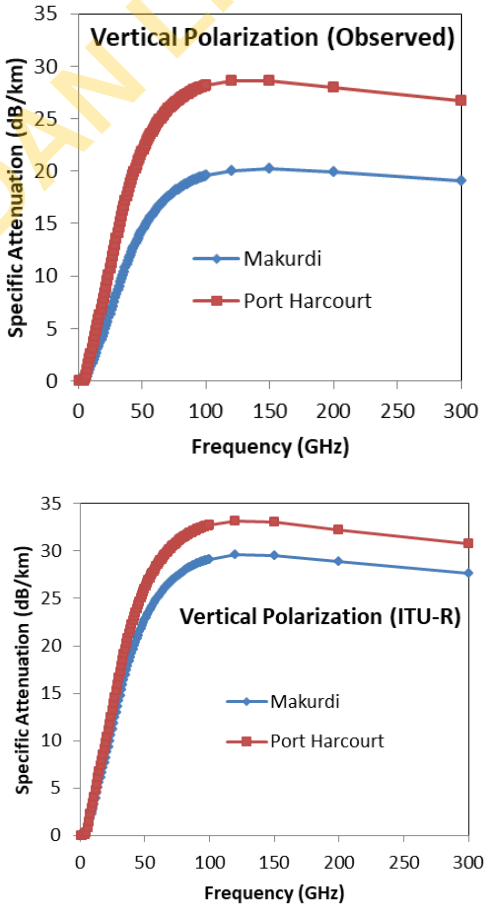

Figure7: Specific rain attenuation versus frequency for vertical polarization using observed and ITU-R rain rate data

Like in other studies (e.g Sakir 2014), Fig 6 show a sharp rapid increase in attenuation below 50 GHz. This is followed by a gradual increase between 50 to 100 GHz, and thereafter remains almost constant for the rest of the frequencies up to 150 GHz after which it begins to decrease

gradually. The gradual increase in attenuation per km is attributed to the lack of synchronization between the signal wavelength and the rain drop size after 50 GHz. The decrease in specific attenuation after 150 GHz is more pronounced at the coastal station (Port Harcourt) than in the semi-arid (Makurdi) station for both horizontal and vertical polarization. From Figs 6 & 7, the specific attenuation of vertical polarization is 0.60dB lower compared to the highest 28.73 dB observed specific attenuation of horizontal polarization at 100 GHz at the coastal station. Similarly, the predicted specific attenuation of vertical polarization by ITU-R is 0.754dB lower than the 33.464 dB specific attenuation of horizontal polarization at 100 GHz. In the semi-arid region (Makurdi), the specific attenuation of vertical polarization is 0.35 dB lower compared to the 19.90 dB specific attenuation of horizontal polarization. Also, The ITU-R predicted specific attenuation of vertical polarization is 0.64 dB lower compared to specific attenuation of horizontal polarization at 100 GHz. It is evident from these figures that, for both the coastal and semi-arid areas, the ITU-R predicted specific attenuation for horizontal polarization and vertical polarization are higher compared to the measured rain rate. The difference in attenuation by horizontal polarization and vertical polarization has been attributed to the distortion in rain drops (Okumara et al.,2010). Rain drops are not spherical but asymmetrical about the horizontal plane, generally with flattened base for large drops (Magono, 1954) as is the case with tropical rains. However, the ITU-R prediction indicates a closer margin in the specific attenuation of the two regions. It should be noted that there is a slight difference between the specific attenuation at the horizontal polarization and the vertical polarization. This finding agrees with the work of Okamura (1961), Olubunmi (2006) and Shayea et al., (2018).

The specific attenuation for each of the years considered for this study was also computed up till the 150GHz frequency threshold at 0.01% of time. Figure 8 show the specific attenuation for each of the years and their average year values. Also shown in Fig 8 are the ITU-R predicted values. The specific attenuation for horizontal and vertical polarization for each year and the corresponding ITU-R average year values at 0.01% of time are presented in Tables 4, 5 and 6. It is observed from Fig 8 and Tables 4, 5 and 6 that at the coastal station, the ITU-R predicted specific attenuation at horizontal polarization and vertical polarization at 50, 100, 120 and 150 GHz is higher for all the years except the year 2008 which has the same value with the observed. Similarly, the ITU-R overestimated the specific attenuation at horizontal and vertical polarization at these frequencies at the semi-arid station for all the years except 2008.

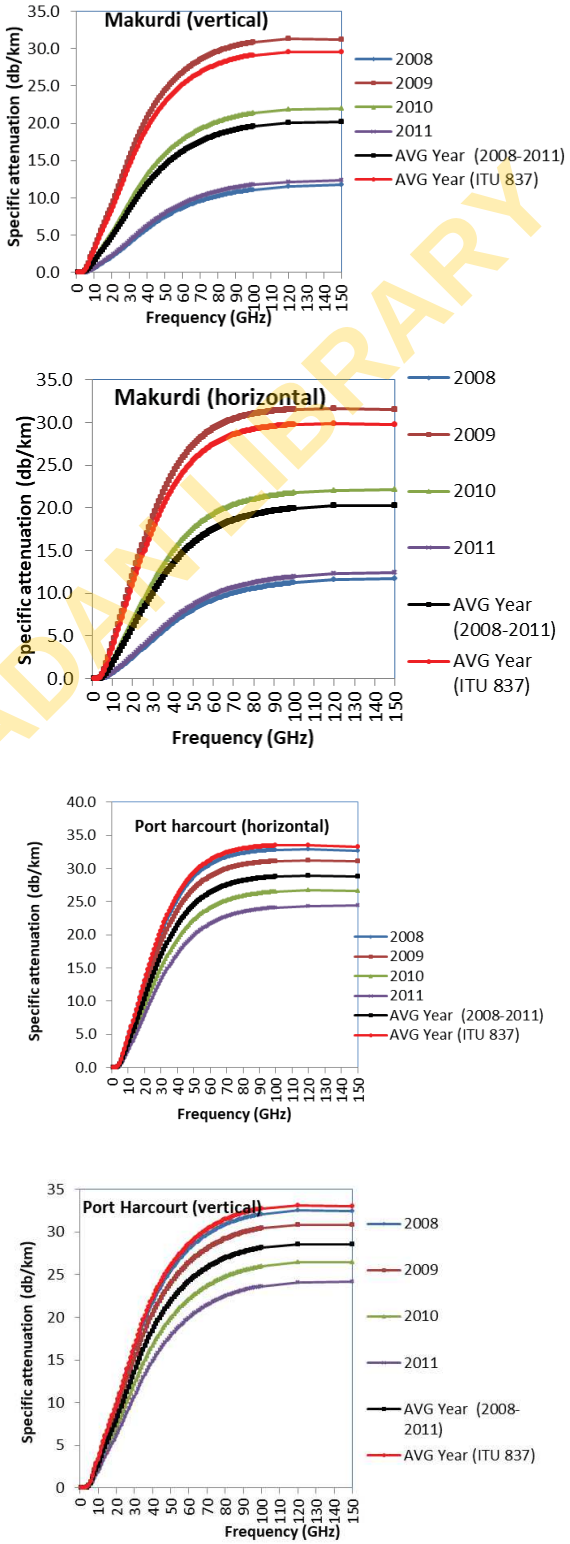

Figure 8: Specific attenuation by rain at 0.01% of time for Makurdi and Port Harcourt

Table 4: Specific attenuation (dB)at 50 GHz and 0.01% of time.

			γ_H			
Year	2008	2009	2010	2011	Av. Year	ITU-R
PH	29.304	26.869	22.227	19.877	24.471	29.304
Mak	8.616	27.311	17.583	8.616	15.847	25.509
			γ_V			
PH	26.002	23.896	19.866	17.819	21.818	26.002
Mak	7.896	24.279	15.814	7.896	14.291	22.718

Table 5: Specific attenuation (dB) at 100 GHz and 0.01% of time.

			γ_H			
Year	2008	2009	2010	2011	Av.Year	ITU-R
PH	33.469	31.104	26.507	24.125	28.747	33.464
Mak	11.924	31.536	21.756	11.924	19.930	29.771
			γ_V			
PH	32.710	30.419	25.954	23.638	28.131	32.710
Mak	11.744	30.838	21.333	11.744	19.555	29.125

Table 6: Specific attenuation (dB) at 150 GHz and 0.01% of time.

			γ_H			
Year	2008	2009	2010	2011	Av.Year	ITU-R
PH	32.700	31.100	26.681	24.392	28.826	33.316
Mak	11.800	31.484	22.103	12.462	20.332	29.803
			γ_V			
PH	32.423	30.819	26.480	24.217	28.599	33.033
Mak	11.700	31.224	21.954	12.409	20.202	29.564

Table 7: ITU-R estimate of specific rain attenuation at the study area

Makurdi						
Frequency	**Horizontal Polarization (dB/km)**			**Vertical Polarization (dB/km)**		
	Derived	ITU-R	Diff.	Derived	ITU-R	Diff.
10	3.50	1.50	2.00	2.50	1.50	1.00
20	10.50	6.50	4.00	8.00	5.00	3.00
30	17.50	10.50	7.00	14.00	8.50	5.50
40	22.50	14.00	8.50	19.00	12.50	6.50
50	25.50	16.50	9.00	22.50	15.00	7.50
60	27.50	18.50	9.00	25.00	17.00	8.00
70	28.50	19.50	9.00	26.50	18.00	8.50
80	29.00	20.00	9.00	28.00	19.20	8.80
90	29.50	20.50	9.00	28.50	20.00	8.50
100	29.90	21.00	8.90	29.00	20.20	8.80
120	20.30	29.90	9.60	20.00	29.60	9.60
150	20.33	29.80	9.47	20.20	29.56	9.36

Frequency	Port Harcourt					
10	3.00	5.0	2.00	2.50	3.5	1.00
20	11.00	13.0	2.00	7.80	9.8	2.00
30	17.50	20.50	3.00	14.00	17.00	3.00
40	22.50	26.00	3.50	19.50	22.50	3.00
50	25.50	29.50	4.00	23.00	26.00	3.00
60	27.50	31.50	4.00	25.00	28.50	3.50
70	28.50	32.50	4.00	25.60	30.00	3.50
80	29.00	33.00	4.00	28.00	31.50	3.50
90	29.50	33.20	3.70	28.50	32.00	3.50
100	29.80	33.50	3.70	29.00	32.50	3.50
120	28.90	33.50	4.60	28.60	33.10	4.50
150	28.83	33.32	4.49	28.60	33.03	4.43

As shown from Figure 8, the highest specific attenuation of 32.7dB at horizontal polarization occured in Port Harcourt, the coastal region at rain rate of about 106.5mm/hr in 2008while the lowest specific attenuation of 11.8dB/km at horizontal polarization ocured in Makurdi, the semi-arid region at rain rate of about 22.0mm/hr in 2008. The specific attenuation on the average year was 28.83dB/km and 20.33db/km in the coastal region and semi-arid region respectively while the ITU-R predicted specific attenuation at horizontal polarization at these regions were was 33.32dB/km and 29.80dB/km respectively. The ITU-R under-estimated specific attenuation in the coastal region at all the frequencies of propagarion while at the semi-arid region it was under-estimated with the 120GHz and 150GHz as the only exception.

3.5.2: Estimating Path Attenuation Using Different Existing Models for Terrestrial Paths

As stated earlier, the rainfall amount along a radio link varies temporally and spatially. As a result, the specific attenuation based on the average rain rate statistics becomes inadequate for attenuation determination along a radio link path (Crane, 1996; Hall et al., 1996;Olubunmi2006). In a bid to quantify the path attenuation by rainfall on communication signals, some authors adopted the use of reduction factor to multiply the measured rain rate at a given point for a given percentage of time while other authors assumed constant rainfall intensity over the signal path hence multiplied the length of the actual path by a reduction coefficient. In this study, the Crane, Moupfouma and ITU-R models are used to determine the path attenuation at the study sites. The choice of these models was based on their good performance in tropical and sub-tropical environment (Fasuyiet, al., 2007).

Fig 9 presents the attenuation per distance at 0.01% of time at the coastal and semi-arid stations. It compares the performance of the Crane and Moufouma models with the ITU-R model for predicting path attenuation. It is observed first that at both stations, the ITU-R provided the lowest estimate of the path attenuation. Second, the Moupfouma model exhibited a linear relationship between attenuation and distance at the two stations. The Crane model seem to be more sensitive to rain intensity considering the fact that rainfall is more in Portharcourt than Makurdi. For example, from Fig 9, the Crane model over estimated path attenuation by about 18.77% in Makurdi and under estimated path attenuation in Portharcourt by 33.02% at 10 km distance. The adequacy of the ITU-R model in estimating path attenuation of radio links is consistent with works in other parts of the world (Fasiuyiet, al., 2007; Sakir, 2014).As averred by Kestwal (2014), rain attenuation degrades system performance and limits the usage of higher frequencies for terrestrial Line Of Sight (LOS) communication systems. Furthermore, Olsen (1999) stressed on the imperative of accurate prediction. Hence, the ITU-R model is preferred over other models for terrestrial paths for path attenuation determination over the study sites at threshold frequencies of 120 and 150 GHz.

Considering the estimation of lowest attenuation by ITU-R, in comparison to Moupfouma and Crane Global model (Figure 9), the ITU-R model (equation 13) was adopted in the estimate of the path attenuation over the frequency thresholds of 120 and 150 GHz at the coastal and semi-arid regions respectively. The path attenuation was plotted at the maximum recommended path length of 60km by ITU-R (ITU-R P. 530-17, 2017) while for maximum millimetric path length of 20 km (Owolawi, 2006; Perlman, 1995; Shebani et al, 2017) the path attenuation was deduced. Figure 10 shows the plot of path attenuation across all the two regions at their observed and ITU-R predicted specific attenuation frequency threshold.

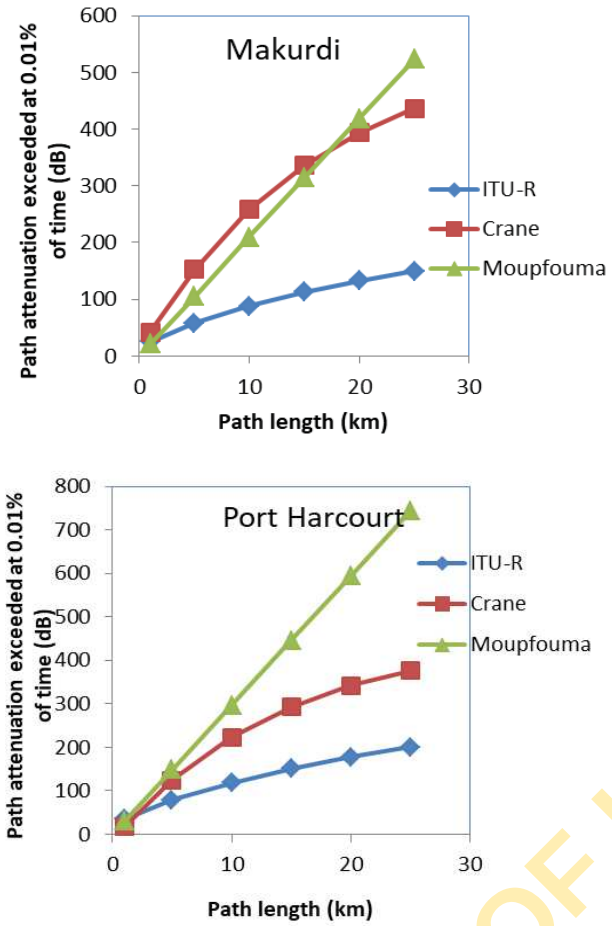

Figure 9: Millimetric Path attenuation exceeded at 0.01% for the Coastal and semi-arid region for horizontal polarization

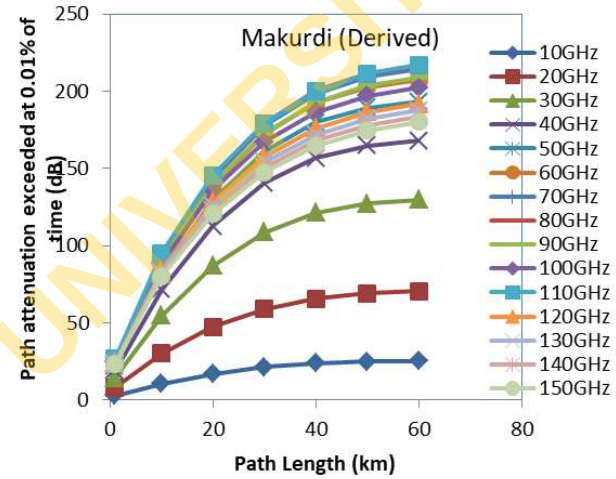

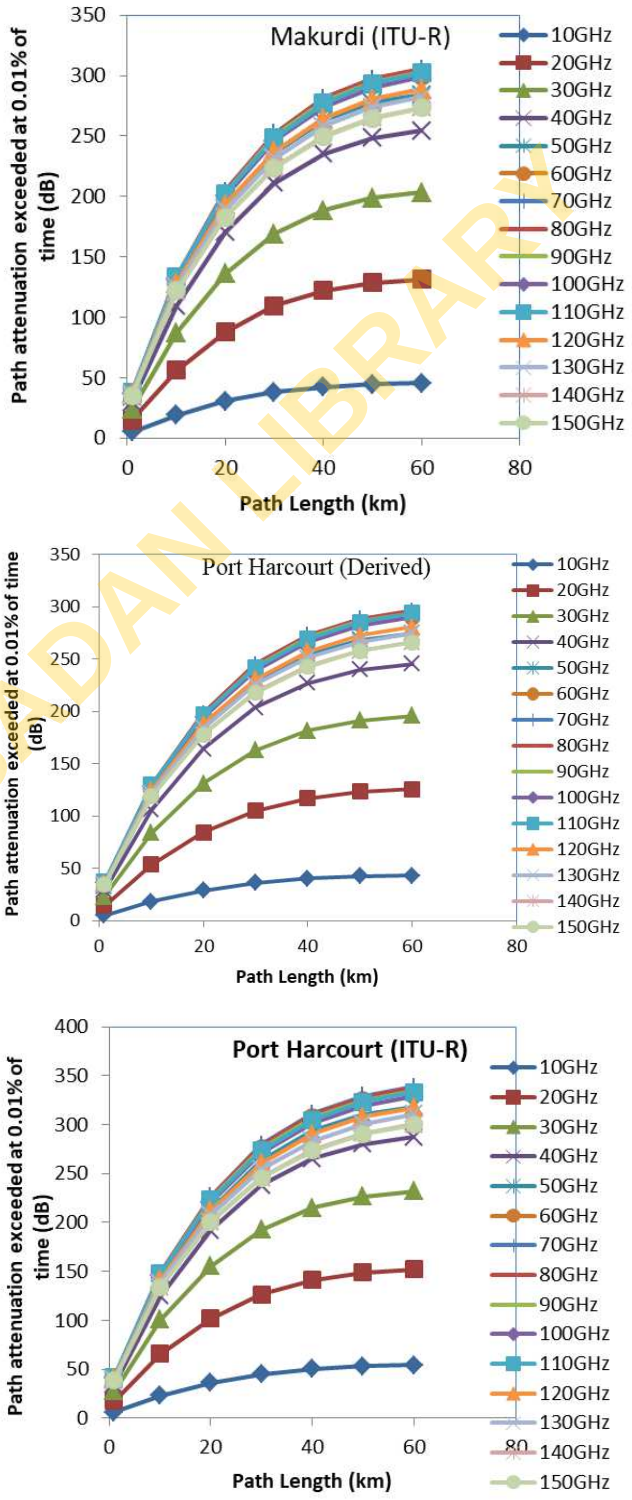

Figure 10: Path attenuation at 0.01% exceedance from derived and ITU-R rain rate predictions for horizontal polarization

As shown from Figure 10, the maximum frequency for clear signals transmission at Port Harcourt, the coastal region is 40 GHz. At high frequency beyond 40GHz, the transmitted signal suffers from overlap. Hence, for transmission at millimetric waveband at this region, the frequency limits are 30 and 40 GHz. These frequencies are equivalent to the upper limit of Ka frequency band and lower limit of V- frequency band (COST Action 280, 2001). The path attenuation exceeded at 20 km path length at 0.01% in this region at 30GHz is 130.91dB while at 40GHz, the path attenuation is 165.00dB, at this region. At Makurdi, the maximum frequency for clear signals transmission is 45GHz. Hence the limits of transmission at millimetric band for these locations are 30GHz to 45GHz. At 0.01% exceedance, the path attenuation at 20km path length at 30GHz band was 85.00dB while at 45GHz, the path attenuation is 122.02dB.

When plotted at 5 GHz interval (not shown), the path attenuation by ITU-R predicted rain rate at 20km path length, clear signal occurred at 30 to 40GHz band in Port Harcourt. At Makurdi, the clear signal band occurred at 30 GHz band only because the 45 GHz band overlapped with the 150 GHz with path attenuation of 185 dB. However, the ITU-R over predicted the value of attenuation at 20km path length at the 40Ghz threshold frequency band by 13.16% and 35.29% at the coastal and semi-arid locations respectively.

3.5.3: Path Attenuations at the 40GHz and 45GHz frequency bands

At the 30-300GHz millimeter wave bands, the frequency threshold of the specific attenuation for the horizontal and vertical polarization at 0.01% of rain rate for the two regions considered ranged from 120GHz to 150GHz. At these frequency thresholds, the highest frequency band without overlaps at 20km path length (Figure 10) were 40GHz and 45GHz respectively. These are the frequency threshold for millimetric communication equipment design for these regions in Nigeria. The path attenuation from derived rain rate and ITU-R predicted rain rate for the two regions at 40GHz and 45 GHz frequency band is presented in Table 8. Figs 11 and 12 is the comparison of the derive path attenuation with the predicted values by ITU-R at these frequencies. The margin between the ITU-R and the derived values at the coastal station is smaller compared to that at the semi-arid station.

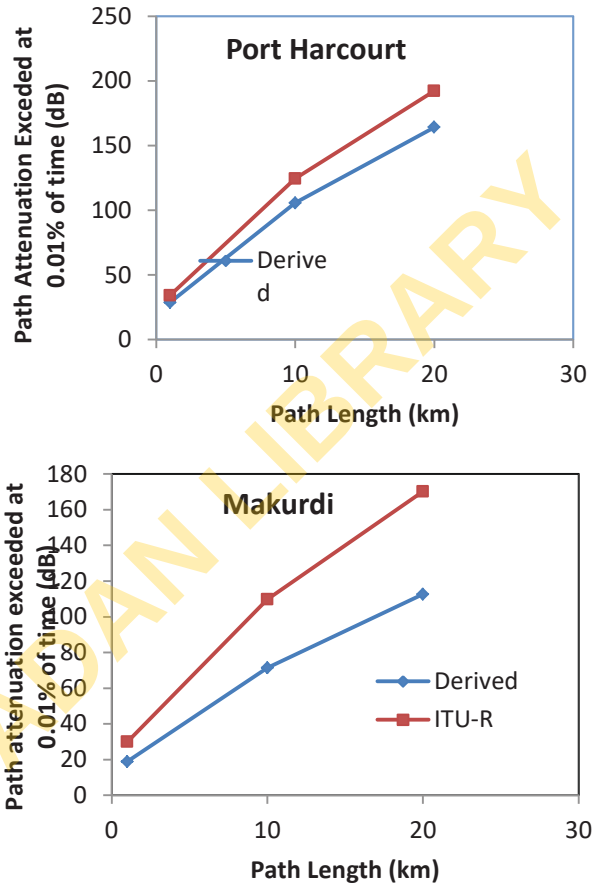

Figure 11:Comparison of derived and ITU-R path attenuation at 40 GHz and at 0.01% at the coastal and semi-arid regions

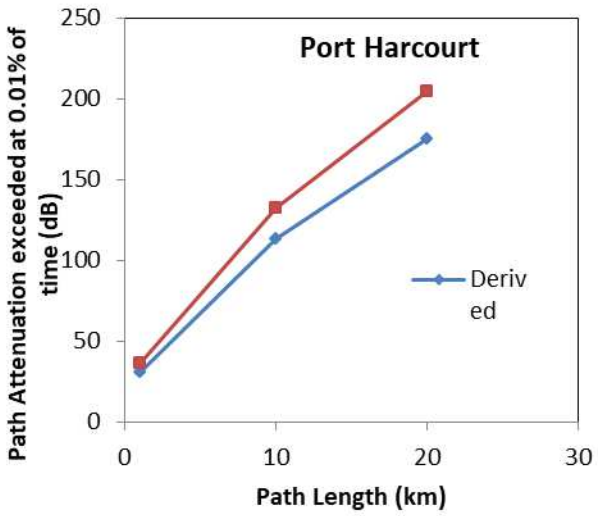

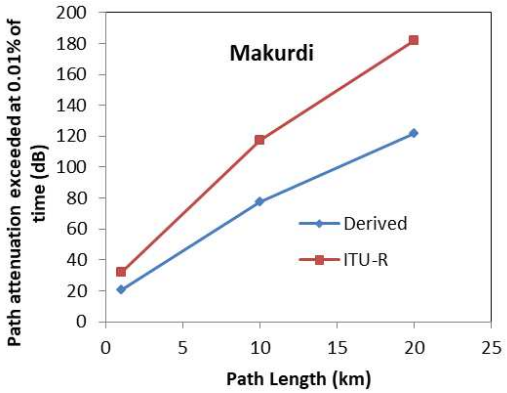

Figure 12: Same as in Fig. 11 but at 45 GHz

Table 8: Path attenuation for 40 GHz and 45 GHz frequency bands at 0.01%

Locations	Path Attenuation at 40GHz band (dB)		Path attenuation at 45GHz band (dB)	
	Derived	ITU-Predicted	Derived	ITU-Predicted
Makurdi	112.58	170.20	122.02	181.83
Port Harcourt	164.14	192.18	175.57	204.43

As shown in the table, the predicted path attenuation by the ITU differs remarkably from the value derived from the measured rain rate at the 40GHz and 45GHz frequency bands. The ITU-R model over estimated path attenuation by 33.85% and 32.89% at 40 and 45 GHz respectively at Makurdi. In PortHartcout, the ITU-R model over estimated path attenuation by 14.59% and 14.12% at these respective frequencies. As stated earlier, rainfall is not the same in all months but varies from month to month as shown in Figs 1 and 2. The proper fade margin is provided by determining the attenuation for each month. Fig. 13 shows the monthly variation of attenuation in horizontal polarization at frequencies from 10 to 150 GHz.

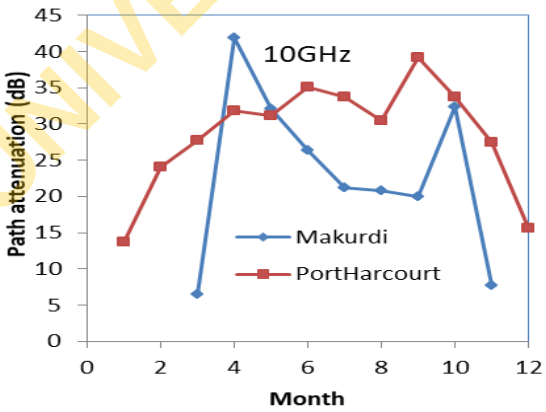

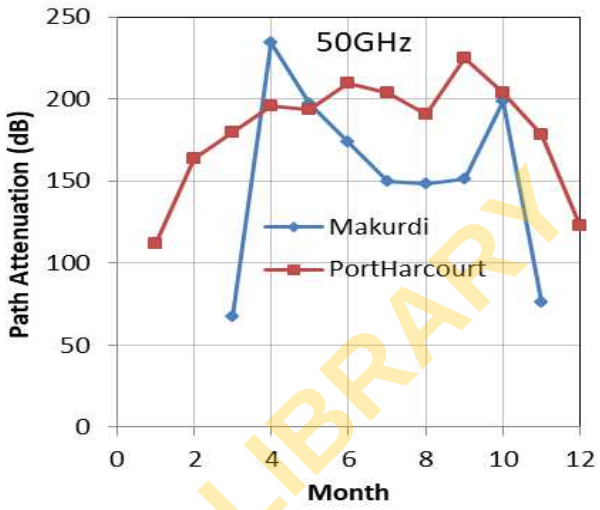

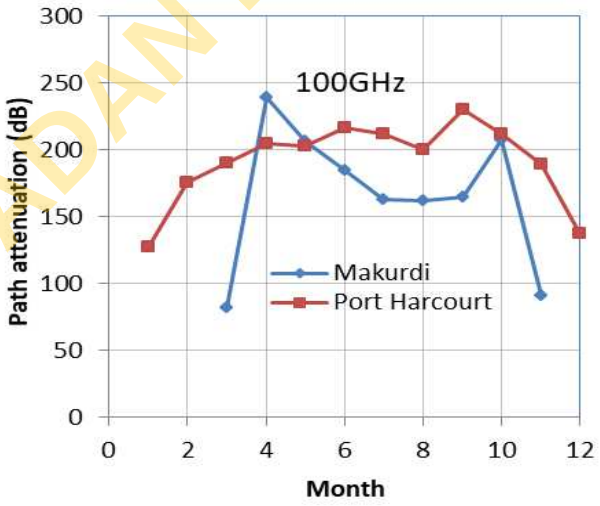

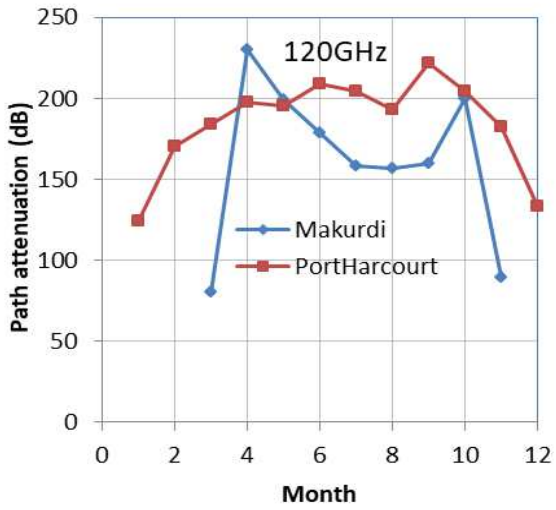

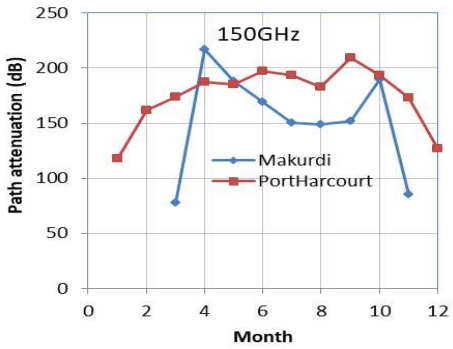

Fig. 13: Monthly variation of path attenuation.

From Fig 13, it can be observed that with the exception of the 10 GHz frequency band, the path attenuation for the semi-arid region flattens out between July and September and reaches a second peak in October for all the frequencies considered. This period coincides with the 'little dry season' (called August break) experienced in the southern part of the country from late July to middle of August. This is the reason for the decreased value of path attenuation at the coastal region in August. Table 9 show the minimum and maximum path attenuation values at these respective frequencies.

Table 9: Monthly minimum and maximum path attenuation for various frequencies

Freq (GHz)		10	50	100	120	150
Station						
Makurdi	Minimum	6.48	67.55	82.09	80.77	77.47
	Maximum	41.85	234.64	239.05	230.16	217.22
PortHarcourt	Minimum	13.66	112.21	129.15	124.05	118.24
	Maximum	39.15	224.64	230.33	221.94	209.59

The monthly path attenuation values at 0.01% of time and at 20 km at these respective frequencies for the two regions are presented in Tables 10 and 11. The zero values in the first two months of the semi-arid station is due to the absence of rain at this period of the year at the station.

Table 10: Path attenuation at 0.01% at 20km path length, for the semi-arid station (Makurdi)

Month	50GHz	100GHz	120GHz	150GHz
3	67.54959	82.08606	80.76937	77.46812
4	234.6428	239.0506	230.1584	217.216
5	197.2865	206.1655	199.1282	188.3836
6	173.7264	184.9341	179.0335	169.6678
7	150.0299	163.1249	158.3358	150.349
8	148.4891	161.6892	156.9711	149.0736
9	151.5629	164.5512	159.6912	151.6155
10	198.6293	207.3633	200.2603	189.437
11	76.25191	91.15654	89.51657	85.73477

Table 11: Path attenuation at 0.01% at 20km path length, Port Harcourt

Month	50GHz	100GHz	120GHz	150GHz
1	112.208	127.1509	124.0493	118.2404
2	163.5667	175.6437	170.224	161.4505
3	179.4035	190.0886	183.9169	174.2195
4	195.9393	204.9624	197.9909	187.3253
5	193.2314	202.5404	195.7008	185.1939
6	209.2191	216.7669	209.1435	197.6982
7	203.9573	212.1039	204.7398	193.6036
8	190.505	200.0965	193.3893	183.0423
9	224.6394	230.3297	221.9397	209.587
10	203.9573	212.1039	204.7398	193.6036
11	177.9925	188.8099	182.7057	173.0908
12	122.6239	137.2218	133.668	127.2629

IV. CONCLUSION

The rain attenuation at the coastal and semi-arid regions has been investigated in this study. In determining the appropriate prediction model for these regions, the Crane Global model, Moupfouma and the ITU-R models were used. The Moupfouma model shows a linear behaviour in the two regions while the Crane model tended towards the ITU-R model in the coastal region. The Crane model over estimated path attenuation by 18.77% and 33.02% at 10 km distance at the semi-arid and coastal stations. The threshold clear band signal frequencies were determined to be 40 and 45 GHz at the two locations. At these respective frequencies, the ITU-R over estimated path attenuation by 33.85% and 32.89% at Makurdi while at Portharcourt, the overestimated values were 14.59% and 14.12% respectively. The highest specific attenuation at horizontal polarization at the 0.01% of time occurred in 2008 with a value 29.30dB at

the coastal station. The minimum path attenuation at the horizontal polarization of 8.62 dB also occurred in 2008 but at the semi-arid station. Overall, the ITU-R overestimated the average year specific attenuation at the two regions. It is believed that the information provided here can be useful for the design of equipment for the 5th Generation Technology.

V. ACKNOWLEDGMENT

The results presented in this paper rely on TRODAN data collected and managed by the Centre for Atmospheric Research, National Space Research and Development Agency, Federal Ministry of Science and Technology, Anyigba, Nigeria. We thank the Centre and their partners for promoting high standards of atmospheric observatory practice as well as the Federal Government of Nigeria for continuous funding of the Nigerian Space programme (www.carnasrda.com).

REFERENCES

1. Abdulrahman Y. A., Islam R. and Rahman T.A. (2012), "An improved ITU-R rain attenuation prediction model over terrestrial microwave links in tropical region,"EURASIP Journal onWireless Communications and Networking, vol. 2012, article 189, 2012.
2. Adeyemi B, Aro T.O. (2004). Variation in surface .water vapour density over four Nigeria Stations. Nig. J. Pure Appl. Phys. 3:46-55.
3. Ajayi,G.O, Feng, S., Radicella, S.M.and Reddy B.M. (Ed) (1996): HandBook on Radiopropagation related to Satellite communications in Tropical and Subtropical Countries. ICTP, Trieste, Italy pp.2-14
4. Ali, A.A., Alhadier, M.A., and Shatila, M.A. (1986). Rain map for radiowave propagation design in Soudi Arabia, International Journal of Infrared and Millimeter wave , vol, 7, no. 11, pp. 1777-1793.
5. Bhartia, P, Bahl, I.J. (1984).Millimeter Wave Engineering and Applications,John Wiley &Sons, New York, Chapter 3 & 4.
6. Bryant G.H., Adimula I.A. and Riva C. (1998).Rain cell diameter and heights. A new model of attenuation presented in URSI Comm F, Aveiro, Portugese.
7. Chebil, J. and Rahman T. A. (1999). Development of 1-minute rain rate contour maps for microwave application in Malaysia Peninsula,Electronic Letters, Vol. 35, 1712-1774.
8. Crane R.K. (1996): Electromagnetic Wave Propagation through Rain, John Wiley, New York, 1996, Chapterl, 2,3,4.
9. Chun O.W. and MandeepJ. S., "Empirical methods for converting rainfall rate distribution from several higher integration times into a 1-minute integration time in Malaysia", GEOFIZIKA, Vol. 30 ,2013.
10. Cost Action 280(2001). Propagation Impairment Mitigation for Millimetre wave radio systems. www.cost280.rl.ac.uk
11. Das S. and MaitraA. (2010).Rain Attenuation modelling in the 10-100GHz frequency using drop size distributions for different climate zones in tropical India.Progress in Electromagnetic Research B, vol.25, p. 211-224.
12. Da Silva MelloLAR, MS Pontes, RM De Souza, NA Perez Garcia (2007) Prediction of rain attenuation in terrestrial links using full rainfall rate distribution. Electron Lett. 43(25), pp. 1442–1443.
13. Diba F.D. (2017). Radio wave propagation modelling under precipitation and clear- air under microwave and millimetric bands over wireless links in the horn of Africa (PhD thesis).
14. Emmanuel I., AdeyemiB. andAdedayo, K. D. (2013). Regional variation of columnar refractivity with meteorological variables from climate monitoring satellite application facility (CM SAF) data over Nigeria. International Journal of Physical Sciences, Vol. 8(17), pp. 825-834.
15. Flavin RK.(1981) Rain attenuation considerations for satellite paths.Report No. 7505, Telecomm.Australia Research Laboratories.
16. Fashuyi M.O. and Afullo T.J. (2007). Rain attenuation prediction and modelling for line of sight links on terrestrial paths in South Africa. Radio Science, vol. 42, doi:10.1029/2007RS003618.
17. Fashuyi M.O. and Afullo T.J. (2007). Rain attenuation prediction and modelling for line of sight links on terrestrial paths in South Africa. Radion Science, vol. 42, doi:10.1029/2007RS003618.
18. Federal Communications Commission (FCC, 1997). Millimeter Wave Propagation: Spectrum Management Implications.Bulletin Number 70.
19. Ghiani, R., L. Luini, and A. Fanti (2017). A Physically based rain attenuation model for terrestrial links. Radio Science (AGU).doi:10.1002/2017R5006320. Green, H. E. (2004), Propagation impairment on Ka-band SATCOM links in tropical and equatorial regions, IEEE Antennas Propag. Mag., 46(2), 31– 44.
20. Godara D.R., Purohit J.S., SandeepRankawatandS.K.Modi (2013). Effect of Foliage Length on Signal Attenuation in Millimeter Band at 35GHz Frequency.International Journal of Computer Applications (0975 – 8887) Volume 84 – No 2.
21. HallM.P.M., Barclay L.W. and HewittM.T (1996).Propagation ofRadiowaves,IEEE, London United kingdom, Chapter 1 and Chapter 4.
22. Ibe O. and Nymphas E.F. (2010).Temperature variations and their effects on rainfall in Nigeria.Global Warming, Green Energy and Technology.Published by Springer Science Business

Media.http://www.springerlink.com/content/rx58w574 87544021/.di
23. Ibe O., Nymphas, E.F. (2017). Characteristics of worst hour rainfall rate for radio wave propagation modelling in Nigeria. MeteorolAtmosPhys 131, 251–261 (2019) https://doi.org/10.1007/s00703-017-0548-3
24. Ibe O. and Nymphas E. F. (2020).Characterization of tropical rainfall structure for some selected locations in Nigeria (In Print)
25. Ito C. and Y. Hosoya, (2006).Proposal of a global conversion method for different integration timerain rates by using M distribution and regional climatic parameters," Electronics and Communications in Japan, Part 1, Vol. 89, No. 4.
26. ITU-R 837-1,2,3,4(2003), Characteristics of Precipitation for Propagation modelling, Recommend. 837-1, ITU-R P Ser., Int. Telecom. Union, Geneva.
27. ITU-R P837-7 (2017).Characteristics of Precipitation for Propagation Modelling, Vol. 2012, P Series, International Telecommunication Union, Geneva, Switzerland.
28. ITU-R P.530-17 (2017). Prediction methods and Propagation data required for the design of terrestrial line-of-sight systems. P Series, International Telecommunication Union, Geneva, Switzerland.
29. Joo, H. L., S. K. Yang, H. K. Jong, and S. C. Yong, (2002).Empirical conversion process of rain rate distribution for various integration times,"Proc. URSI Commission F Wave Propagationand Remote Sensing, 1450-1454, Maastricht.
30. Karmakar P.K., LahariSengupta, Maiti M. and Carlos Frederico Angelis (2010). Some of the atmospheric influences on microwave propagation through atmosphere. American
31. Journal of Scientific and Industrial Research1(2): 350-358.
32. Kestwal, C.K., Joshi, S. and Garcia, L.S. (2014). Prediction of Rain Attenuation and Impact of Rain in Wave Propagation at Microwave Frequency for Tropical Region (Uttarakhand, India), International Journal of Microwave Science and Technology, Volume 2014, Article ID 958498, 6 pages.
33. Lavergnat J. and Gole P. (1998).A stochastic raindrop time distribution model. American Meteorological society, p.805-818.
34. Magono, C. (1954) On the shape of water drops falling in stagnant air. J. Meteorol. 11,77–79.
35. Marcus M. andPatta B. (2005), "Millimeter Wave propagation-Spectrum Management Implications," IEEE Microwave Magazine, Vol. 6, No2, pp. 54- 61.
36. Moupfouma, F. and L. Martin (1995).“Modelling of the rainfall ratecumulative distribution for the design of satellite and terrestrialcommunication systems,” Int. J. of Satellite Comm., Vol. 13, No. 2, 105–115.
37. Moupfouma F. (1984). "Improvement of a Rain Attenuation prediction Method forTerrestrial Microwave Links,"IEEE Transactions on Antennas and Propagation,Vol. AP-32, No. 12, pp. 1368-1372
38. Moupfouma, F. (2009), Electromagnetic waves attenuation due to rain: A prediction model for Terrestrial or L.O.S SHF and EHF radio communication links, J. Infra, Milli., TetrahertzWaves, 30(6), 622 – 632.
39. Nandi D and Maitra A. (2019). Effects of Rain on millimeter wave communication for tropical region, URSI AP-RASC 2019. New Delhi, India, ursi.org/proceedings/procAP19/papers2019/ManuscriptDaliaAPRASC2019.pdf (Accessed, October, 2019)
40. Ojo J.S, Adenugba AK and Adediji AT (2016).Dynamical Model for deriving 1-Min Rain Rate from Various Integration Times in a Tropical Region.Journal of Telecommunications System & Management, Volume 5 • Issue 1 • 1000127.
41. Okamura, S., Funakawa, K., Uda, H., Kato, J. and Oguchi, T. (1961) Effect of polarization on the attenuation by rain at millimeter-wave length. J. Radio Res. Labs. (Japan) 8,73–80.
42. Okamura S. and Oguchi T. (2010).Electromagnetic wave propagation ion in rain and polarization effects. Proceedings of the Japan Academy.Series B, Physical and Biological Sciences. P. 539-562. Doi: 10.2183/pjab.86.539.
43. Okamura, S., Funakawa, K., Uda, H., Kato, J. and Oguchi, T. (1961) Effect of polarization on the attenuation by rain at millimeter-wave length. J. Radio Res. Labs. (Japan) 8,73–80.
44. Olubunmi O.O (2006). A study of rain attenuation on terrestrial paths at millimetric wavelengths in South Africa.MSc thesis, Electrical Engineering, University of Nwazu Natal.
45. Olsen, R. L. (1999), Radioclimatological modeling of propagation effects in clear-air and precipitation conditions: Recent advances and future directions, in Proceedings of Radio Africa “99 Conference, pp. 92 – 106, Gaborone, Botswana.
46. Olsen, R. L., D. V. Rogers, and D. B. Hodge (1978), The aRb relation in the calculation of rain attenuation, IEEE Trans. Antennas Propag., 26(2), 547 – 556.
47. Owolawi P. A., Afullo T. J. andMalinga S. J. (2009). Effect of Rainfall on Millimeter Wavelength Radio in Gough and Marion Islands. Progress In Electromagnetics Research Symposium, Beijing, China, p. 91-98.
48. Owolawi P. A.,Malinga S. J. and Afullo T. J. (2012).Estimation of Terrestrial Rain attenuation at microwave and millimeter wave signals in South Africa using the ITU-R model. Progress in Electromagnetics Research Symposium, p. 952-962.
49. Owolawi P. A., Afullo T. J. andMalinga S. J. (2008). Rainfall Rate Characteristics for the Design of

Terrestrial Link.http://satnac.org.za/proceedings/2008/papers/access/Owolawi%20No%2035.pdf [Accessed 24 October, 2015]
50. Owolawi P.A. (2006). Rain rate and Rain Drop Size distribution Models for Line-of-Sight Millimetric system in South Africa. M.Sc. Thesis .Electrical Engineering Department, University of Kwazu-Natal.
51. Prassana A. (2008). Understanding Millimeter Wave and Wireless Communication.Loea Corporation, San Diego.
52. Perlman B.S. (1995), "Millimeter-Wave Technology," A Tutorial given at the FCC, Sept. 6.
53. Shebani N. M., kaeib A. F., and Zerek A. R. (2017). Estimation of rain attenuation based on ITU-R model for terrestrial link in Libya. www.researchgate.net/publications (accessed April, 2018)
54. Ramakrishna K., Punyaseshudu, D. (2014). Estimation of rain induced Specific attenuation. International Journal of Scientific Engineering and Technology. Volume No.3 Issue No.2, pp : 144 – 146.
55. Rao P.R. (2010). Role of mm waves in Terrestrial and satellite communications. International Journal of systems and technologies, vol. 3, No. 1, p.25-34.
56. Sakir H. (2014). Rain attenuation prediction for terrestrial microwave link in Bangladesh. Journal of Electrical and electronics Engineering, vol. 7, No.1. p. 63-68.
57. Segal, B. (1986) .The influence of raingage integration time on measured rainfall-intensity distribution functions," J. of Atmospheric and Oceanic Tech., Vol. 3, 662-671.
58. Skolnik M.I. (1970) ."Millimetre and sub millimetre wave applications," Proceedings of the symposium on Sub-millimeter waves, Polytechnic Press of Poly. Institute of Brooklyn, New York, pp9-25.
59. Semire,F.A., Mokhtara R.M., Omotosho T.V., Ismaila W., Mohamada N., and. Mandeep J.S. (2012). Analysis of Cumulative Distribution Function of 2-year Rainfall Measurements in Ogbomoso, Nigeria.International Journal of Applied Science and Engineering 2012. 10, 3: 171-179.
60. ShayeaIbraheem , Abd, RahmanTharek , HadriAzmiMarwan andArsadArsany (2018). Rain attenuation of millimetre wave above 10 GHz for terrestrial links in tropical regions.
61. Wiley Online Library, https://doi.org/10.1002/ett.3450.
62. Shebani N. M., kaeib A. F., and Zerek A. R. (2017). Estimation of rain attenuation based on ITU-R model for terrestrial link in Libya. www.researchgate.net/publications (accessed April, 2018)
63. Sulochana Y., Chandrika P. and Rao S.V.B (2014).Rain rate and rain attenuation statistics for different homogenous regions in India. Indian Journal of Radio and space physics, vol. 43, p. 303-314.
64. Vaclav K. and Martin G. (2010).Rain Attenuation on Terrestrial Wireless Links in the mmFrequency Bands, Advanced Microwave and Millimeter Wave Technologies Semiconductor Devices Circuitsand Systems, Moumita Mukherjee (Ed.), ISBN: 978-953-307-031-5.
65. Zhang, W., and N. Moayeri (1999), Power-Law Parameters of Rain Specific Attenuation, Rep. IEEE, 802.16 WG, 1 – 8..